nature materials

LETTERS

PUBLISHED ONLINE: 7 DECEMBER 2015 | DOI: 10.1038/NMAT4492

Strong interplay between stripe spin fluctuations, nematicity and superconductivity in FeSe

Qisi Wang[1], Yao Shen[1], Bingying Pan[1], Yiqing Hao[1], Mingwei Ma[2], Fang Zhou[2], P. Steffens[3], K. Schmalzl[4], T. R. Forrest[5], M. Abdel-Hafiez[6,7], Xiaojia Chen[6], D. A. Chareev[8], A. N. Vasiliev[9,10,11], P. Bourges[12], Y. Sidis[12], Huibo Cao[13] and Jun Zhao[1,14]*

In iron-based superconductors the interactions driving the nematic order (that breaks four-fold rotational symmetry in the iron plane) may also mediate the Cooper pairing[1]. The experimental determination of these interactions, which are believed to depend on the orbital or the spin degrees of freedom[1-4], is challenging because nematic order occurs at, or slightly above, the ordering temperature of a stripe magnetic phase[1,5]. Here, we study FeSe (ref. 6)—which exhibits a nematic (orthorhombic) phase transition at $T_s = 90$ K without antiferromagnetic ordering—by neutron scattering, finding substantial stripe spin fluctuations coupled with the nematicity that are enhanced abruptly on cooling through T_s. A sharp spin resonance develops in the superconducting state, whose energy (∼4 meV) is consistent with an electron–boson coupling mode revealed by scanning tunnelling spectroscopy[7]. The magnetic spectral weight in FeSe is found to be comparable to that of the iron arsenides[8,9]. Our results support recent theoretical proposals that both nematicity and superconductivity are driven by spin fluctuations[1,10–13].

The vast majority of the parent compounds of the iron-based superconductors exhibit a stripe-type long-range antiferromagnetic (AFM) order which is pre-empted by an electronic nematic order[1]. In analogy to the nematic phase of liquid crystal, which is characterized by molecules that have no positional order but tend to be aligned in the same direction; electronic nematicity is an electronic phase that spontaneously breaks the rotational symmetry while preserving the translation symmetry. The superconductivity in these materials, which is unconventional in nature, emerges when the magnetic and nematic order are partially or completely suppressed by chemical doping or by the application of pressure[1,5]. The stripe AFM order consists of columns of parallel spins along the orthorhombic *b* direction, together with antiparallel spins along the *a* direction. Similar to the stripe AFM order, the nematic order also breaks the four-fold rotational symmetry, which is signalled by the tetragonal to orthorhombic structure phase transition and a pronounced in-plane anisotropy of electronic and magnetic properties[1,5,14–17]. It has been proposed that the nematicity is driven either by orbital or spin fluctuations, where the orbital fluctuation mechanism produces a sign-preserving s^{++}-wave pairing, whereas the spin fluctuation mechanism favours a sign-changing $s^{\pm}$-wave or *d*-wave pairing[1–5,13,18,19]. However, as orbital and spin degrees of freedom are coupled and could be easily affected by the nearby stripe magnetic order, an identification of the primary driving force of the nematicity remains elusive[1–4,13,18].

The iron-chalcogenide compound FeSe ($T_c \approx 8$ K), which possesses the simplest crystal structure of all the iron-based superconductors (Fig. 1a), exhibits a variety of exotic properties that are unprecedented for other iron-based superconductors. For example, the T_c of FeSe increases to ∼40 K under pressure[20] or by ion/molecule intercalation[21]. In addition, the T_c of single-layer FeSe thin film is as high as 100 K, which is vastly superior to other iron-based superconductors[22]. More importantly, unlike most iron-based materials, the tetragonal to orthorhombic structural transition in bulk FeSe is not followed by a stripe magnetic order[6]. This provides an excellent opportunity to elucidate the microscopic origin of the nematicity and its interplay with superconductivity. The absence of stripe magnetic order in FeSe seems to cast doubt on the spin-driven nematicity scenario. Moreover, recent nuclear magnetic resonance (NMR) measurements suggested that there were almost no spin fluctuations above T_s in the tetragonal phase, which was interpreted as a breakdown of the spin scenario[23,24]. However, NMR probes momentum-integrated spin fluctuations only at very low energies (∼0.1 μeV or lower), whereas the momentum dependence of the higher-energy spin fluctuations has yet to be determined. Crucially, it is these spin fluctuations, especially at the energy scale close to the superconducting gap, that are believed to be important in driving the superconductivity and nematicity[10,13]. This issue can be addressed by inelastic neutron scattering measurements which can probe spin fluctuations over a wide range of momentum and energy.

The superconducting properties of our FeSe single crystals (see Methods) were characterized by DC magnetic susceptibility and resistivity measurements, which gave an onset T_c of 8.7 K with a transition width of ∼0.3 K, indicating their high quality (Fig. 1b,c). Moreover, clear kinks in the magnetic susceptibility and resistivity associated with the tetragonal to orthorhombic structure transition were also observed close to 90 K. We first use

[1]State Key Laboratory of Surface Physics and Department of Physics, Fudan University, Shanghai 200433, China. [2]Beijing National Laboratory for Condensed Matter Physics, Institute of Physics, Chinese Academy of Science, Beijing 100190, China. [3]Institut Laue-Langevin, 71 Avenue des Martyrs, 38042 Grenoble Cedex 9, France. [4]Juelich Centre for Neutron Science JCNS Forschungszentrum Juelich GmbH, Outstation at ILL, 38042 Grenoble, France. [5]European Synchrotron Radiation Facility, BP 220, 38043 Grenoble Cedex, France. [6]Center for High Pressure Science and Technology Advanced Research, Shanghai 201203, China. [7]Faculty of Science, Physics Department, Fayoum University, 63514 Fayoum, Egypt. [8]Institute of Experimental Mineralogy, Russian Academy of Sciences, Chernogolovka, Moscow District 142432, Russia. [9]Low Temperature Physics and Superconductivity Department, M.V. Lomonosov Moscow State University, Moscow 119991, Russia. [10]Theoretical Physics and Applied Mathematics Department, Ural Federal University, Ekaterinburg 620002, Russia. [11]National University of Science and Technology "MISiS", Moscow 119049, Russia. [12]Laboratoire Leon Brillouin, CEA-CNRS, CEA-Saclay, 91191 Gif sur Yvette, France. [13]Neutron Scattering Science Division, Oak Ridge National Laboratory, Oak Ridge, Tennessee 37831-6393, USA. [14]Collaborative Innovation Center of Advanced Microstructures, Fudan University, Shanghai 200433, China. *e-mail: zhaoj@fudan.edu.cn

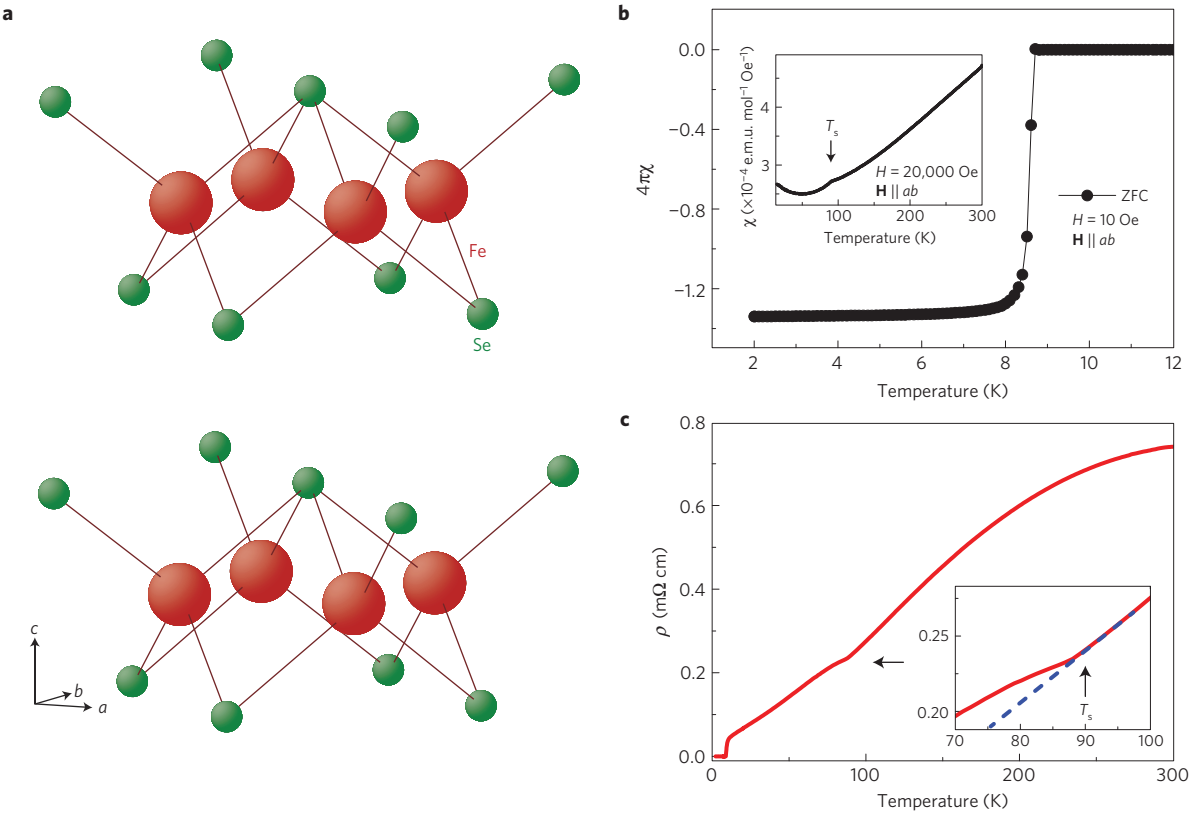

Figure 1 | Orthorhombic crystal structure, magnetic susceptibility, χ, and resistivity, ρ, of FeSe single crystal. a, Schematic diagram of FeSe crystal structure. **b**, DC magnetic susceptibility measurements on the single-crystalline FeSe sample. A sharp superconducting transition is observed at $T_c = 8.7$ K in the zero-field-cooled (ZFC) measurement in a magnetic field of $H = 10$ Oe, indicating ~100% exclusion of the external magnetic field. The screening is slightly larger than −1 because of the demagnetization effect. The inset shows the susceptibility measured in a magnetic field of $H = 20$ kOe. The magnetic fields are applied perpendicular to the c axis. **c**, In-plane resistivity as a function of temperature. The inset shows data around $T_s = 90$ K on an enlarged scale. The blue dashed line is a linear extrapolation of the data above T_s.

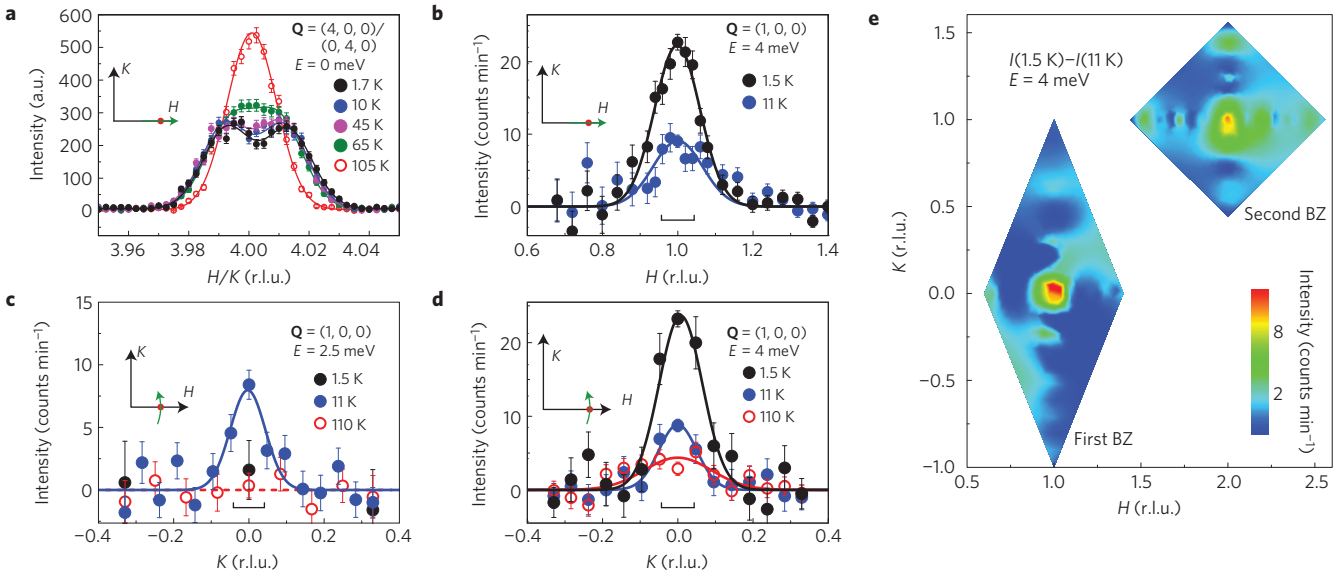

Figure 2 | Structure phase transition and momentum dependence of the spin fluctuations at various temperatures in FeSe. We present the data by defining the wavevector **Q** at (q_x, q_y, q_z) as $(H, K, L) = (q_x a/2\pi, q_y a/2\pi, q_z c/2\pi)$ reciprocal lattice units (r.l.u.) in the orthorhombic unit cell. **a**, Temperature dependence of the transition from the tetragonal to orthorhombic symmetry; the figure shows the splitting of the (4, 0, 0)/(0, 4, 0) nuclear reflections. **b**–**d**, **Q**-scans near (1, 0, 0) at various energies and temperatures; linear backgrounds are subtracted (see Supplementary Information). The scan directions are marked by green arrows in the insets. The fitted peak centre at 4 meV and 1.5 K is $\mathbf{Q} = (0.998 \pm 0.003, 0.008 \pm 0.007, 0)$—that is, commensurate within the error bars. The horizontal bars indicate the instrument resolution. **e**, 2D contour plot of the temperature difference scattering $[S(1.5\,\mathrm{K}) - S(11\,\mathrm{K})]$ interpolated from a series of **Q**-scans at 4 meV. Error bars indicate 1 s.d. BZ, Brillouin zone.

elastic neutron scattering (see Methods) to study the structural and magnetic ordering properties of FeSe. These measurements clearly resolved the splitting of the (4, 0, 0)/(0, 4, 0) peaks below $T_s = 90$ K (Fig. 2a); this is indicative of the structural phase transition from the tetragonal to orthorhombic symmetry. On the other hand, no magnetic Bragg peaks associated with the stripe or double stripe magnetic order were observed (not shown) at temperatures down to 1.5 K, consistent with previous measurements of powder samples[6]. Instead, in the inelastic channel, we have observed strong spin fluctuations near (1, 0, 0), which corresponds to the stripe AFM wavevector of the parent compounds of iron-based superconductors[5]. To determine the momentum dependence of the spin fluctuations and their interplay with superconductivity, we have performed a series of rocking/transverse and radial/longitudinal **Q**-scans (the scan directions are perpendicular and along **Q**, respectively) above and below T_c. As shown in Fig. 2b,d, representative **Q**-scans at 4 meV are commensurate near (1, 0, 0) at $T = 11$ K, for both the transverse and longitudinal directions, and show no observable anisotropy. Furthermore, the peak intensity is drastically enhanced below T_c, which is reminiscent of the magnetic resonant mode that has been observed in other iron-based superconductors[5,8,9,13,25,26]. Conversely, the scattering at 2.5 meV is suppressed on entering the superconducting state owing to the opening of the superconducting spin gap (Fig. 2c). The redistribution of the magnetic spectral weight across T_c clearly indicates that the spin fluctuations near (1, 0, 0) are closely related to superconductivity. To clarify the effects of superconductivity on these spin fluctuations, we have subtracted the signal at 4 meV of the normal state from that of the superconducting state and plotted its detailed momentum structure as a 2D contour map (Fig. 2e). The outcome shows that the spin fluctuation spectra are commensurate, with little anisotropy (within our instrumental accuracy). In addition to the results shown near (1, 0, 0), we also performed similar measurements in the second magnetic Brillouin zone (BZ) centred at (2, 1, 0) associated with the stripe magnetic structure (Fig. 2e). A similar signal is also observed, but with weaker intensity owing to the decreased magnetic form factor. These results unambiguously demonstrate that this scattering is from pure magnetic fluctuations that are associated with the stripe magnetism, and not from phonons.

Figure 3 summarizes the energy dependence of the dynamic spin correlation function $S(\mathbf{Q},\omega)$ at $\mathbf{Q} = (1,0,0)$ for three temperatures (1.5, 11 and 110 K). The figure confirms that the spectral weight loss in the superconducting spin gap (<3 meV) is compensated by a sharp resonance mode at around 4 meV. Moreover, the detailed temperature dependence of the scattering at 4 meV shows an order-parameter-like behaviour, which is clearly coupled to the onset of superconductivity (Fig. 4a). The spin resonance mode has been interpreted either as a spin exciton within the superconducting gap, which arises from scattering between portions of the Fermi surface where the superconducting gap function has an opposite sign[13], or as a broad hump structure induced by an overshoot in the magnetic spectrum above the superconducting gap in a sign-preserving s^{++} pairing state[19]. The sharp mode that we observed here is consistent with the spin exciton model, as the mode energy (4 meV) is below the superconducting gap ($2\Delta \approx 5$ meV; ref. 27). Furthermore, the energy width (~1.2 meV) of this mode is essentially resolution-limited and much sharper than in other iron-based superconductors[5,8,9,13,25,26]. Finally, the resonance energy ($E_r = 4$ meV $\approx 5.3 k_B T_c$) is consistent with the electron boson coupling mode (~3.8 meV) revealed by scanning tunnelling spectroscopy[7], thereby suggesting a strong coupling between the electrons and spin fluctuations. These results are consistent with a spin-fluctuation-mediated sign-changing pairing mechanism, but not the orbital-fluctuation-mediated sign-preserving s^{++}-wave pairing mechanism[13,19,28].

Although the commensurate stripe spin fluctuations persist at all temperatures measured, the system still remains paramagnetic to low temperatures. Theoretically, it has been shown that the magnetic interactions in FeSe are more frustrated than in iron arsenides, therefore preventing long-range magnetic order[10–12]. Hence, it is informative to compare the magnetic spectral weight in FeSe with that of iron arsenide superconductors. To this end we have calculated in absolute units the imaginary part of the dynamic susceptibility $\chi''(\mathbf{Q},\omega)$ by normalizing $S(\mathbf{Q},\omega)$ for the thermal population factor and the intensity of acoustic phonons (Fig. 3b and Supplementary Information). The result gives an integrated resonance spectral weight (~$0.00212\mu_B^2$/Fe) that is approximately 30% of that in the carrier-doped $BaFe_{1.85}Co_{0.15}As_2$ ($E_r = 9.5$ meV) (ref. 8), but twice as large as the damped resonance mode in the isovalently doped $BaFe_{1.85}Ru_{0.15}As_2$ ($T_c = 14$ K, $E_r = 5.5$ meV; ref. 9). As the T_c (8.7 K) of FeSe is also about a factor of three lower than in $BaFe_{1.85}Co_{0.15}As_2$ ($T_c = 25$ K), the overall magnetic spectral weights in both systems are comparable.

Having established the interplay between the spin fluctuations and superconductivity, we now turn to the impact of nematicity on the spin fluctuations. Previous NMR measurements suggested the absence of spin fluctuations above T_s in the tetragonal phase[23,24]. By contrast, our neutron scattering measurements show substantial spin fluctuations in the tetragonal phase ($T = 110$ K; Figs 3a and 2d). What is more, the energy dependence of the dynamical spin correlation function $S(\mathbf{Q},\omega)$ exhibits a spin-gap-like feature at low energies at $T = 110$ K (Fig. 3a), which is confirmed by

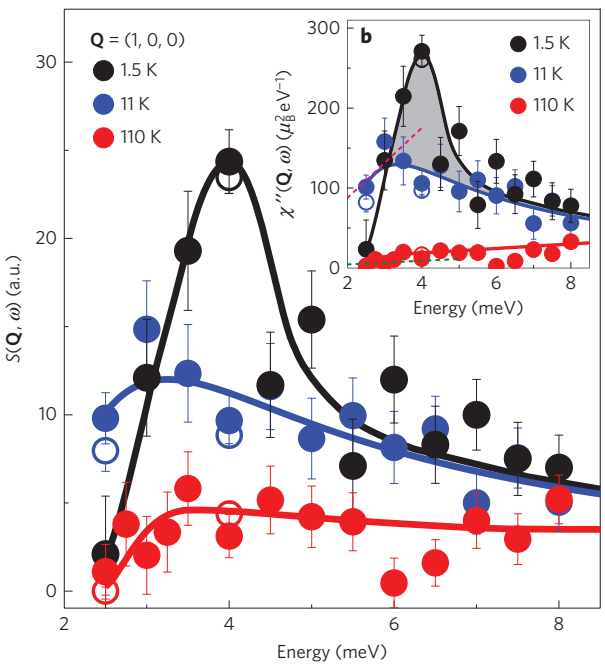

Figure 3 | Energy dependence of spin fluctuations for FeSe in the superconducting state ($T = 1.5$ K) and normal state ($T = 11$ and 110 K). **a**, Energy dependence of the dynamic spin correlation function $S(\mathbf{Q},\omega)$ at $\mathbf{Q} = (1,0,0)$ after a background correction. The background is measured at $\mathbf{Q} = (0.944, 0.330, 0)$ and $\mathbf{Q} = (0.944, -0.330, 0)$, which are on both sides of the magnetic peak in the rocking scan (see Fig. 2c,d and the Supplementary Information). The open circles are data fitted with **Q**-scans. **b**, Energy dependence of the imaginary part of the dynamic susceptibility $\chi''(\mathbf{Q},\omega)$. The data are obtained from $S(\mathbf{Q},\omega)$ by correcting for the Bose-population factor and are normalized to absolute units with acoustic phonons as described in the Supplementary Information. The solid curves are guides to the eye. The shaded area denotes the resonance spectral weight. The dashed lines indicate the slope of $\chi''(E)/E$ for $E \to 0$, which is related to the spin-lattice relaxation rate measured by NMR. Error bars indicate 1 s.d.

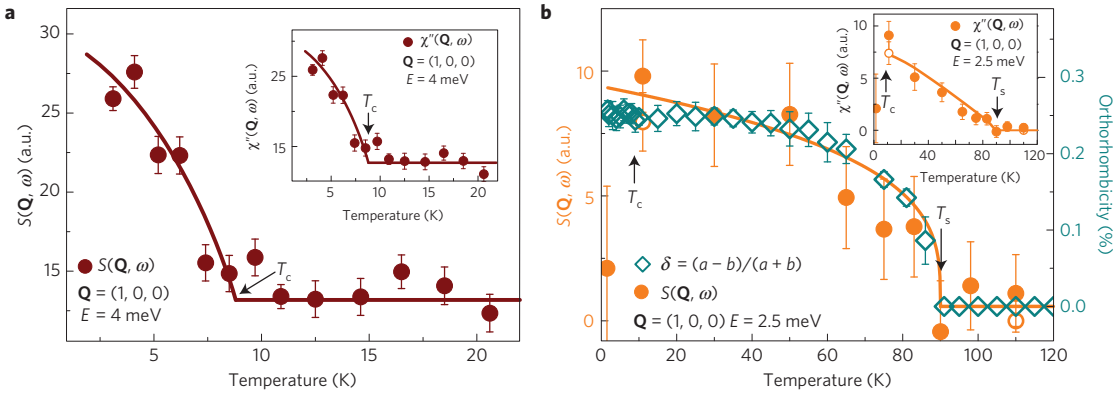

Figure 4 | Temperature dependence of spin fluctuations in FeSe. a, Temperature dependence of the dynamic spin correlation $S(\mathbf{Q},\omega)$ at $E=4$ meV, which clearly shows a kink at T_c. The inset shows the temperature evolution of $\chi''(\mathbf{Q},\omega)$. **b**, Temperature dependence of $S(\mathbf{Q},\omega)$ at $E=2.5$ meV and the orthorhombicity $\delta(T)=(a-b)/(a+b)$ shows an order-parameter-like behaviour with an onset at T_s. The orthorhombicity is determined by the high-resolution neutron diffraction data in Fig. 2a and Supplementary Fig. 5. The temperature dependence of the orthorhombicity near T_s can be fitted by a simple power law $\delta(T)=\delta_0(1-T/T_s)^{\beta}$, where $\beta=0.303\pm0.034$. Although NMR measurements have demonstrated the competition between nematicity and superconductivity in FeSe (ref. 24), the suppression of orthorhombicity below T_c is not clearly observable for our neutron data, probably owing to the intrinsic weak effect and resolution constraint. We note that the decrease of the scattering intensity at 2.5 meV and 1.5 K is due to the opening of the superconducting spin gap (Fig. 3). The suppressed spectral weight at 2.5 meV is compensated by the resonance mode at 4 meV, so the total spectral weight exhibits only a weak change across T_c. Therefore, this does not conflict with the very weak suppression of the orthorhombicity below T_c in the spin-driven nematicity scenario. The inset shows the temperature evolution of $\chi''(\mathbf{Q},\omega)$, which also exhibits a kink at T_s. The open circles are data fitted with **Q**-scans. The solid lines are a guide to the eye. Error bars indicate 1 s.d.

the featureless **Q**-scan at 2.5 meV (Fig. 2c). These results agree with a theoretically predicted gapped nematic quantum paramagnetic state, where frustrated magnetic correlation is the driving force of the nematicity and is responsible for the lack of long-range magnetic order in FeSe (ref. 10). This naturally accounts for the absence of low-energy spin fluctuations above T_s suggested by NMR measurements[23,24]. The most striking observation is that the spin fluctuations are enhanced abruptly in the orthorhombic phase at $T=11$ K (Fig. 3a). We note that the spin fluctuation enhancement is more pronounced at lower energies, suggesting a slowing down of spin fluctuations. This indicates that the system is closer to the stripe magnetic ordered state at low temperature. To determine if the increase of the spin fluctuation is indeed associated with the nematic order, we carefully measured the temperature dependence of the scattering at 2.5 meV, which is the lowest energy that can be measured in our thermal triple-axis spectrometer with a reasonable background. Intriguingly, a comparison of the temperature evolution of $S(\mathbf{Q},\omega)$ with the orthorhombicity $\delta(T)=(a-b)/(a+b)$ reveals that the enhancement of $S(\mathbf{Q},\omega)$ is clearly coupled to the development of the nematic (orthorhombic) phase (Fig. 4b). These results are consistent with the recent proposals (based on either itinerant or local moment pictures) that the nematic order is driven by spin fluctuations[1,10–12]. In a local moment model where frustrated magnetic interactions drive nematic order in FeSe, the magnetic frustration is lifted by the onset of the orthorhombic distortion, thus causing the system to move towards a stripe ordered phase. As a result the spin fluctuations at the stripe ordering wavevector are enhanced.

It is informative to compare the spin fluctuations of FeSe with that of the iron selenide superconductors with a higher T_c, but without nematic order. The low-energy spin fluctuations in $FeTe_{1-x}Se_x$ ($T_c=14$ K) and $Rb_xFe_{2-y}Se_2$ ($T_c=32$ K) appear at $\mathbf{Q}=(1,-0.3\le\xi\le0.3)$ and $\mathbf{Q}=(1,\pm0.5)$, respectively[25,26,29]. Different from FeSe, the dynamic spin correlation $S(\mathbf{Q},\omega)$ of $FeTe_{1-x}Se_x$ exhibits little temperature dependence from T_c to 300 K (ref. 25). Moreover, the spin fluctuations of $FeTe_{1-x}Se_x$ are broad and incommensurate/anisotropic[25,26], in contrast to the relatively sharp and commensurate spin fluctuations at the stripe AFM wavevector in FeSe. Therefore, FeSe is closer to the stripe magnetic instability and consequently has a larger spin–spin correlation length. These results further imply that the nematicity is driven by stripe spin fluctuations, although superconductivity can be mediated by spin fluctuations either at or away from the stripe AFM wavevector.

In summary, we have reported evidence of strong coupling between the stripe spin fluctuations, nematicity and superconductivity in single-crystalline FeSe. Contrary to earlier NMR measurements[23,24], our neutron scattering data reveal substantial commensurate stripe spin fluctuations in the tetragonal phase, which are coupled with orthorhombicity and are abruptly enhanced in the nematic phase. This is not predicted in a simple orbital-driven nematicity model[24]. Moreover, a resolution-limited sharp spin resonance appears well below the superconducting gap and is coupled with the electronic density of states, indicating a spin-fluctuation-mediated sign-changing pairing symmetry rather than an orbital-fluctuation-mediated sign-preserving s^{++}-wave pairing symmetry. These results are in agreement with the theoretical predictions that nematicity and superconductivity are driven by spin fluctuations[1,10–13], and are critical in identifying the microscopic paring mechanism of this system. The elucidation of the interplay between spin fluctuations, nematicity and superconductivity will also have important implications for the understanding of other exotic properties of iron selenide superconductors, such as the drastically increased T_c under substrate strain/external pressure or by ion/molecule intercalation[20–22].

Methods

Methods and any associated references are available in the online version of the paper.

Received 4 March 2015; accepted 26 October 2015; published online 7 December 2015; corrected online 15 December 2015

References

1. Fernandes, R. M., Chubukov, A. V. & Schmalian, J. What drives nematic order in iron-based superconductors? *Nature Phys.* **10,** 97–104 (2014).
2. Fang, C., Yao, H., Tsai, W.-F., Hu, J. & Kivelson, S. A. Theory of electron nematic order in LaFeAsO. *Phys. Rev. B* **77,** 224509 (2008).

3. Xu, C., Muller, M. & Sachdev, S. Ising and spin orders in the iron-based superconductors. *Phys. Rev. B* **78,** 020501(R) (2008).
4. Kruger, F., Kumar, S., Zaanen, J. & van den Brink, J. Spin-orbital frustrations and anomalous metallic state in iron-pnictide superconductors. *Phys. Rev. B* **79,** 054504 (2009).
5. Dai, P. C., Hu, J. P. & Dagotto, E. Magnetism and its microscopic origin in iron-based high-temperature superconductors. *Nature Phys.* **8,** 709–718 (2012).
6. McQueen, T. M. *et al.* Tetragonal-to-orthorhombic structural phase transition at 90 K in the superconductor $Fe_{1.01}Se$. *Phys. Rev. Lett.* **103,** 057002 (2009).
7. Song, C. L. *et al.* Imaging the electron–boson coupling in superconducting FeSe films using a scanning tunneling microscope. *Phys. Rev. Lett.* **112,** 057002 (2014).
8. Inosov, D. S. *et al.* Normal-state spin dynamics and temperature-dependent spin-resonance energy in optimally doped $BaFe_{1.85}Co_{0.15}As_2$. *Nature Phys.* **6,** 178–181 (2010).
9. Zhao, J. *et al.* Effect of electron correlations on magnetic excitations in the isovalently doped iron-based superconductor $Ba(Fe_{1-x}Ru_x)_2As_2$. *Phys. Rev. Lett.* **110,** 147003 (2013).
10. Wang, F., Kivelson, S. & Lee, D. H. Nematicity and quantum paramagnetism in FeSe. *Nature Phys.* **11,** 959–963 (2015).
11. Glasbrenner, J. K. *et al.* Effect of magnetic frustration on nematicity and superconductivity in iron chalcogenides. *Nature Phys.* **11,** 953–958 (2015).
12. Yu, R. & Si, Q. M. Antiferroquadrupolar and Ising-nematic orders of a frustrated bilinear-biquadratic Heisenberg model and implications for the magnetism of FeSe. *Phys. Rev. Lett.* **115,** 116401 (2015).
13. Scalapino, D. J. A common thread: The pairing interaction for unconventional superconductors. *Rev. Mod. Phys.* **84,** 1383 (2012).
14. Chuang, T.-M. *et al.* Nematic electronic structure in the "parent" state of the iron-based superconductor $Ca(Fe_{1-x}Co_x)_2$ As_2. *Science* **327,** 181–184 (2010).
15. Lu, X. Y. *et al.* Nematic spin correlations in the tetragonal state of uniaxial-strained $BaFe_{2-x}Ni_xAs_2$. *Science* **345,** 657–660 (2014).
16. Yi, M. *et al.* Symmetry-breaking orbital anisotropy observed for detwinned $Ba(Fe_{1-x}Co_x)_2As_2$ above the spin density wave transition. *Proc. Natl Acad. Sci. USA* **108,** 6878–6883 (2011).
17. Chu, J.-H., Kuo, H.-H., Analytis, J. G. & Fisher, I. R. Divergent nematic susceptibility in an iron arsenide superconductor. *Science* **337,** 710–712 (2012).
18. Zhang, Q. *et al.* Neutron-scattering measurements of the spin excitations in LaFeAsO and $Ba(Fe_{0.953}Co_{0.047})_2As_2$: Evidence for a sharp enhancement of spin fluctuations by nematic order. *Phys. Rev. Lett.* **114,** 057001 (2015).
19. Kontani, H. & Onari, S. Orbital-fluctuation-mediated superconductivity in iron pnictides: Analysis of the five-orbital Hubbard–Holstein model. *Phys. Rev. Lett.* **104,** 157001 (2010).
20. Medvedev, S. *et al.* Electronic and magnetic phase diagram of β-$Fe_{1.01}Se$ with superconductivity at 36.7 K under pressure. *Nature Mater.* **8,** 630–633 (2009).
21. Guo, J. G. *et al.* Superconductivity in the iron selenide $K_xFe_2Se_2 (0 \leq x \leq 1.0)$. *Phys. Rev. B* **82,** 180520(R) (2010).
22. Ge, J.-F. *et al.* Superconductivity above 100 K in single-layer FeSe films on doped $SrTiO_3$. *Nature Mater.* **14,** 285–289 (2015).
23. Böhmer, A. E. *et al.* Origin of the tetragonal-to-orthorhombic phase transition in FeSe: A combined thermodynamic and NMR study of nematicity. *Phys. Rev. Lett.* **114,** 027001 (2015).
24. Baek, S.-H. *et al.* Orbital-driven nematicity in FeSe. *Nature Mater.* **14,** 210–214 (2015).
25. Xu, Z. J. *et al.* Local-moment magnetism in superconducting $FeTe_{0.35}Se_{0.65}$ as seen via inelastic neutron scattering. *Phys. Rev. B* **84,** 052506 (2011).
26. Qiu, Y. M. *et al.* Spin gap and resonance at the nesting wave vector in superconducting $FeSe_{0.4}Te_{0.6}$. *Phys. Rev. Lett.* **103,** 067008 (2009).
27. Kasahara, S. *et al.* Field-induced superconducting phase of FeSe in the BCS-BEC cross-over. *Proc. Natl Acad. Sci. USA* **111,** 16309–16313 (2014).
28. Zhang, C. L. *et al.* Distinguishing $s^{\pm}$ and s^{++} electron pairing symmetries by neutron spin resonance in superconducting $NaFe_{0.935}Co_{0.045}As$. *Phys. Rev. B* **88,** 064504 (2013).
29. Park, J. T. *et al.* Magnetic resonant mode in the low-energy spin-excitation spectrum of superconducting $Rb_2Fe_4Se_5$ single crystals. *Phys. Rev. Lett.* **107,** 177005 (2011).

Acknowledgements

We thank D. H. Lee, Q. Si, F. Wang and H. Yao for useful discussions. This work is supported by the National Natural Science Foundation of China (Grant No. 11374059), the Ministry of Science and Technology of China (973 project: 2015CB921302) and the Shanghai Pujiang Scholar Program (Grant No. 13PJ1401100). M.M. and F.Z. acknowledge support from the National Natural Science Foundation of China (Grant No. 11190020). H.C. received support from the Scientific User Facilities Division, Office of Basic Energy Sciences, US Department of Energy. A.N.V. was supported in part by the Ministry of Education and Science of the Russian Federation in the framework of Increase Competitiveness Program of NUST ⟨MISiS⟩ (No. 2-2014-036). D.A.C. and A.N.V. also acknowledge the support of the Russian Foundation for Basic Research through Grants 13-02-00174, 14-02-92002, 14-02-92693.

Author contributions

J.Z. planned the project. M.M., F.Z., D.A.C. and A.N.V. synthesized the sample. Q.W., Y. Shen, B.P., Y.H., M.A.-H. and X.C. characterized the sample. Q.W. and Y. Shen. carried out the neutron experiments with experimental assistance from P.S., K.S., T.R.F., P.B., Y. Sidis and H.C. J.Z. and Q.W. analysed the data and wrote the paper. All authors provided comments for the paper.

Additional information

Supplementary information is available in the online version of the paper. Reprints and permissions information is available online at www.nature.com/reprints. Correspondence and requests for materials should be addressed to J.Z.

Competing financial interests

The authors declare no competing financial interests.

Methods

Neutron scattering studies on FeSe single crystals have been hampered by the lack of high-quality samples with the correct phase. Recently, advances in crystal growth techniques have allowed us to grow FeSe single crystals significantly larger than what was previously available[30,31]. Our single-crystal X-ray diffraction refinements gave a stoichiometric chemical composition [$FeSe_{0.990(10)}$] to within the error bar, and importantly no interstitial atoms or impurity phases were observed. The refined structure parameters are summarized in Supplementary Table 1. We also note that the c axis lattice constant of our sample is longer than that of the Se-deficient sample reported in ref. 32. This is consistent with the positive correlation between the c axis lattice constant and Se concentration[32].

The inelastic neutron scattering measurements were carried out for the neutron energy loss convention (energy is transferred from the neutron to sample) on the IN20 thermal triple-axis spectrometer at the Institut Laue-Langevin, Grenoble, France and the 2T1 thermal triple-axis spectrometer at the Laboratoire Leon Brillouin, France. The FeSe single crystals were co-aligned in the $(H, K, 0)$ horizontal scattering plane within $\sim 3^\circ$ mosaicity for the measurements. The elastic measurements were performed on one piece of small single crystal on the 4F2 cold triple-axis spectrometer at the Laboratoire Leon Brillouin, France (the instrument configurations are described in the Supplementary Information).

Note added in proof: After we finished this paper, we became aware of a related paper describing neutron scattering measurements on FeSe powder samples[33].

References

30. Chareev, D. *et al.* Single crystal growth and characterization of tetragonal $FeSe_{1-x}$ superconductors. *Cryst. Eng. Commun.* **15,** 1989–1993 (2013).
31. Ma, M. W. *et al.* Flux-free growth of large superconducting crystal of FeSe by traveling-solvent floatingzone technique. *Supercond. Sci. Technol.* **27,** 122001 (2014).
32. Hsu, F. C. *et al.* Superconductivity in the PbO-type structure α-FeSe. *Proc. Natl Acad. Sci. USA* **105,** 14262–14264 (2008).
33. Rahn, M. C. *et al.* Strong $(\pi, 0)$ spin fluctuations in β-FeSe observed by neutron spectroscopy. *Phys. Rev. B* **91,** 180501 (2015).